Bioorganic & Medicinal Chemistry 21 (2013) 311–320

Contents lists available at SciVerse ScienceDirect

Bioorganic & Medicinal Chemistry

journal homepage: www.elsevier.com/locate/bmc

Ridaifen B, a tamoxifen derivative, directly binds to Grb10 interacting GYF protein 2

Senko Tsukuda [a], Tomoe Kusayanagi [a], Eri Umeda [b], Chihiro Watanabe [b], Yu-ta Tosaki [b], Shinji Kamisuki [a], Toshifumi Takeuchi [a], Yoichi Takakusagi [a], Isamu Shiina [b], Fumio Sugawara [a,*]

[a] Department of Applied Biological Science, Faculty of Science and Technology, Tokyo University of Science, 2641 Yamazaki, Noda, Chiba 278-8510, Japan
[b] Department of Applied Chemistry, Faculty of Science, Tokyo University of Science, 1-3 Kagurazaka, Shinjuku-ku, Tokyo 162-8601, Japan

ARTICLE INFO

Article history:
Received 31 August 2012
Revised 3 October 2012
Accepted 5 October 2012
Available online 29 October 2012

Keywords:
Ridaifen B
Tamoxifen
Phage display
GIGYF2
Akt

ABSTRACT

Ridaifen B (RID-B) is a tamoxifen derivative that potently inhibits breast tumor growth. RID-B was reported to show anti-proliferating activity for a variety of estrogen receptor (ER)-positive human cancer cells. Interestingly, RID-B was also reported to possess higher potency than that of tamoxifen even for some ER-negative cells, suggesting an ER-independent mechanism of action. In this study, a T7 phage display screen and subsequent binding analyses have identified Grb10 interacting GYF protein 2 (GIGYF2) as a RID-B-binding protein. Using a cell-based assay, the Akt phosphorylation level mediated by GIGYF2 was found to have decreased in the presence of RID-B.

1. Introduction

Tamoxifen (Fig. 1) is an antagonist of the estrogen receptor (ER) and is widely used in hormone therapy and to prevent the recurrence of cancer in patients with ER-positive breast cancers.[1,2] In breast cancer cells, tamoxifen inhibits cell proliferation by blocking growth signals and inducing apoptosis.[3] However, recent reports have shown that tamoxifen induces apoptosis even in ER-negative cells, which suggests that tamoxifen has other target proteins.[4,5] Additionally, tamoxifen can induce some major side effects including a higher incidence of endometrial cancer and drug resistance following long-term therapy.[6,7] In our previous studies we synthesized novel tamoxifen derivatives in order to better understand the mechanism of action of this drug and to generate new therapeutic agents with reduced side effects.[8,9]

Ridaifen B (RID-B), one of these tamoxifen derivatives (Fig. 1), showed a higher inhibitory activity on cellular proliferation than that of tamoxifen. The global anti-tumor activity of RID-B against a variety of human cancer cells showed that RID-B displayed no difference in inhibitory activity between ER-positive and ER-negative cells.[9,10] Furthermore, on an analysis using a COMPARE program, it was suggested that the mode of action for RID-B was different from that for more than 200 of existing drugs for cancer treatment including tamoxifen.[9] These data indicated that there may be an unknown ER-independent mode of action for RID-B.

To identify RID-B-binding proteins, we used a T7 phage display method. Phage display is a powerful technique for identifying peptides or proteins that bind to proteins or small molecules of interest. However, unlike protein samples, passive immobilization of

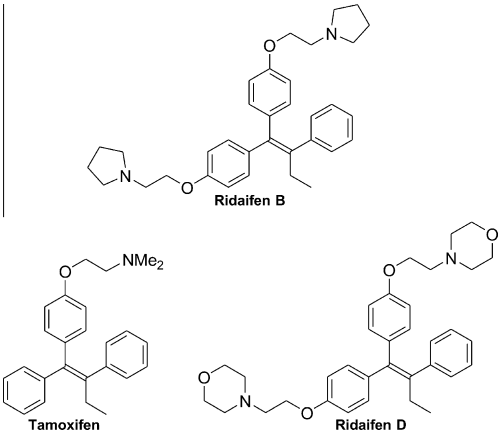

Figure 1. Chemical structures of tamoxifen, RID-B and RID-D.

* Corresponding author. Tel.: +81 471 24 1501x3400; fax: +81 471 23 9767.
E-mail address: sugawara@rs.noda.tus.ac.jp (F. Sugawara).

0968-0896/$ - see front matter © 2012 Elsevier Ltd. All rights reserved.
http://dx.doi.org/10.1016/j.bmc.2012.10.037

small molecules onto a plate surface is generally unsuccessful. Therefore, biotinylated small molecule derivatives and avidin-coated microplates are universally used for affinity selection. A T7 phage display method uses a library constructed from T7 phage particles. Each phage particle expresses peptides of up to about 1200 amino acids in length on the capsid that is identical to proteins or their fragments encoded in living cells or organs.[11–13] Through several rounds of screening, phage particles displaying amino acid sequences that recognize the small molecule of interest are gradually enriched. The amino acid sequences expressed on the capsid of the selected phage particles are then easily identified by sequencing the phage DNA. A subsequent similarity search in the genome database enables a prediction of the potential binding partner(s) as well as the likely binding site. Moreover, unlike many other methods, phage display does not rely on the target protein being soluble and expressed at relatively high levels. Thus, phage display facilitates the identification of less soluble proteins, such as membrane proteins, as well as proteins with a low expression level. In the past several years, we have determined a number of binding partners of small molecules by using a T7 phage display screening protocol.[14–20]

Here we report the identification of Grb10 interacting GYF protein 2 (GIGYF2) as a RID-B-binding protein using a T7 phage display screen. It has been demonstrated that GIGYF2 regulates phosphatidylinositol-3-kinase (PI3K)/Akt signaling pathway of the receptor tyrosine kinase, which is involved in cell proliferation.[21,21] A bead pull-down assay and surface plasmon resonance (SPR) analyses confirmed the direct interaction between RID-B and GIGYF2. Furthermore, using a cell-based assay, the Akt phosphorylation level mediated by GIGYF2 was found to have decreased in the presence of RID-B. These results might explain a possible ER-independent mode of action for RID-B.

2. Results and discussion

2.1. Synthesis of biotinylated RID-B and ridaifen D derivatives

Biotinylated RID-B (Bio-RID-B), 2-[3-(*N*-biotinyl-6-aminohexanoyl)phenyl]-1,1-bis{4-[2-(pyrrolidin-1-yl)ethoxy]phenyl}-1-butene (**7**), was synthesized by the Mukaiyama reductive coupling reaction,[23,24] and the Shiina esterification,[25–27] as shown in Scheme 1. First, 1-[3-(benzyloxy)phenyl]propanone (**2**)[28] was treated with an excess amount of 4,4′-dihydroxybenzophenone (**1**) in the presence of the low-valent titanium species generated from titanium(IV) chloride with zinc powder to afford the desired cross coupling product **3** in 94% yield. The phenol moieties in **3** were transformed into the corresponding aminoethyl ethers by alkylation in 88% yield, and the benzyl protective group in the tetrasubstituted olefin **4** was then cleaved under hydrogenation conditions to provide the phenol derivative **5** in 92% yield. Finally, rapid esterification of *N*-biotinyl-6-aminohexanoic acid (**6**) with the RID-B derivative **5** was carried out in dimethylformamide (DMF) solvent using 2-methyl-6-nitrobenzoic anhydride (MNBA) with 4-(dimethylamino)pyridine (DMAP). The facile dehydration process successfully furnished the probe molecule **7** in 70% yield. It is noteworthy that this is the first application of the MNBA-mediated

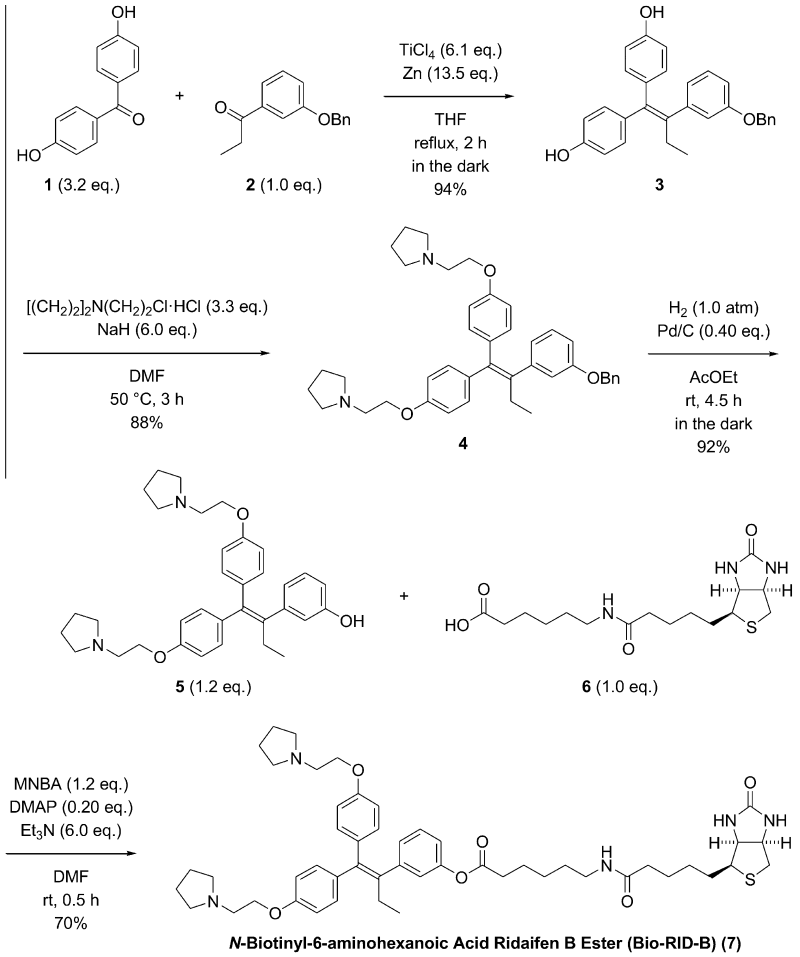

Scheme 1. Synthesis of a biotinylated RID-B derivative (Bio-RID-B) (**7**).

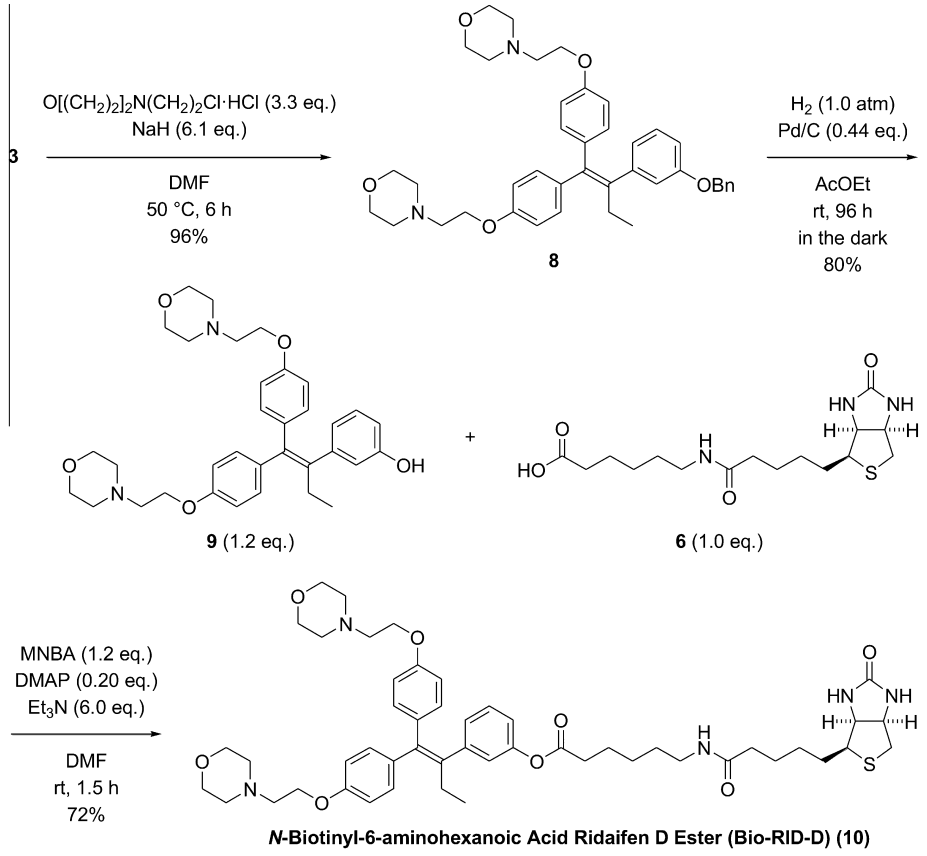

Scheme 2. Synthesis of a biotinylated RID-D derivative (Bio-RID-D) (**10**).

coupling reaction between carboxylic acids and alcohols to the expeditious and effective synthesis of the biotin labeled small molecules.[29,30]

Next, biotinylated RID-D (Bio-RID-D), 2-[3-(*N*-biotinyl-6-aminohexanoyl)phenyl]-1,1-bis{4-[2-(morpholin-4-yl)ethoxy]phenyl}-1-butene (**10**), was also synthesized using a similar procedure as described in Scheme 2. Aminoethyl groups were introduced into the bisphenol **3** in 96% yield, and the phenol derivative **9** was successively prepared from the benzyl ether **8** by hydrogenation in 80% yield. Facile esterification of **6** with the RID-D derivative **9** also took place in the presence of MNBA and DMAP to afford the probe molecule **10** in 72% yield.

2.2. Selection of RID-B-binding protein using a T7 phage display screen

To explore RID-B-binding proteins, we performed a phage display screen. A T7 phage library was constructed from a cDNA library of Jurkat cells, an estrogen receptor-negative human leukemia cell line. First, the T7 phage library was incubated with Bio-RID-B immobilized on streptavidin-coated wells. After incubation, unbound and non-specifically bound phage particles were removed by washing. Finally, the remaining phage particles on the wells were eluted and amplified for the next round. The ratio of recovered phage titer dramatically increased after four rounds of selection, indicating the enrichment of T7 phage particles that potentially bind to RID-B (Fig. 2A). Fifteen individual phage plaques were randomly isolated after the fourth round of selection and the amino acid sequence of the displayed protein was determined. Three out of the 15 phage clones had the same DNA sequence encoding a polypeptide of 286 a.a., whereas the remaining 12 phage clones encoded a polypeptide of 135 a.a. (Table 1). We also

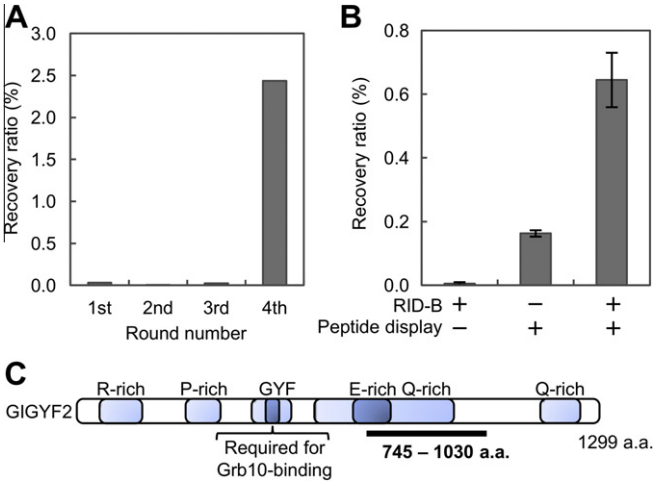

Figure 2. Selection of RID-B-binding protein by a T7 phage display screening procedure. (A) Relative enrichment of T7 phage particles binding to RID-B in each round of selection. The phage titer in the eluate from the Bio-RID-B-immobilized well was compared to the input library titer and shown as recovery ratio. (B) Affinity check of the 286 a.a. phage clone for RID-B. The T7 phage that displays the 286 a.a. [peptide display (+)] or control phage clone [peptide display (−)] was incubated in a well with [RID-B (+)] or without [RID-B (−)] of Bio-RID-B and shown as recovery ratio (%). (C) Schematic representation of full-length GIGYF2. Underline indicates the region that corresponds to the 286 a.a. sequence displayed on the RID-B-binding T7 phage clone.

performed the screening of clones that bind to ridaifen D (RID-D) (Fig. 1), whose cytotoxic activities are lower than that of RID-B, as well as a screen for clones that bind nonspecifically to the control well containing no immobilized small molecule. We obtained two

Table 1
Amino acid sequences and frequency of the phage clones selected from the Bio-RID-B immobilized well

Amino acid sequence	Number of amino acid	Frequency
DPSKGRWVEGITSEGYHYYYDLISGASQWEKPEGFQGDLKKTAVKTVWVEGLSEDGFTYYYNTETGE SRWEKPDDFIPHTSDLPSSKVNENSLGTLDESKSSDSHSDSDGEQEAEEGGVSTETEKPKIKFKEKNK	135	12/15
EMRAKREEEERKRQEELRRQQEEILRRQQEEERKRREEEELARRKQEEALRRQREQEIALRRQREEEERQQQEEA LRRLEERRREEEERRKQEELLRKQEEEAAKWAREEEEAQRRLEENRLRMEEEAARLRHEEEERKRKELEVQR QKELMRQRQQQQEALRRLQQQQQQQQLAQMKLPSSSTWGQQSNTTAEMRAKREEEERKRQEELRRQQE EILRRQQEEERKRREEEELARRKQEEALRRQREQEIALRRQREEEERQQQEEALRRLEERRREEEERRK	286	3/15

After the fourth-round of selection by T7 phage display, 15 single phage clones were randomly picked and their DNA sequences analyzed to determine the phage displayed peptides.

clones from the Bio-RID-D-immobilized well and two clones from the control well. The phage clone displaying a polypeptide of 135 a.a. was observed in the eluate from the control well in addition to the RID-B and RID-D immobilized wells, suggesting this was a nonspecific binding phage clone (Tables 1, S1 and S2).

We decided to check the affinity of the T7 phage displaying the 286 a.a. polypeptide for RID-B. The corresponding T7 phage clone and a control T7 phage clone displaying no peptide were amplified and then separately added to the RID-B-immobilized well or a blank control well. The bound T7 phage particles were then recovered and the ratio of the two phage clones isolated from the RID-B-immobilized well was compared to that from the non-immobilized control well. The recovery ratio of the phage clone displaying the 286 a.a. polypeptide was four-fold higher from the RID-B immobilized well than from the blank control well. Furthermore, the control phage clone did not bind to RID-B. These results indicated that the phage clone displaying the 286 a.a. polypeptide selectively interacts with RID-B (Fig. 2B).

A similarity search using FASTA identified that the 286 a.a. sequence displayed on the RID-B-binding phage clone is identical to the 745–1030 region of Grb10 interacting GYF protein 2 (GIGYF2) (Figs. 2C and S1). It has been reported that GIGYF2 is a protein that interacts with growth factor receptor-bound protein 10 (Grb10) and has a critical role in the PI3K/Akt signaling pathway. However, its molecular function is not fully understood. Despite the high molecular weight of GIGYF2 (1299 a.a.), use of T7 phage display and subsequent similarity search enabled the identification of this protein as a potential RID-B-binding partner along with a candidate binding site in 745–1030. This 286 a.a. sequence did not show any similarity with GIGYF1, an another subtype of GIGYF, indicating that binding of RID-B to GIGYF is specific for subtype2.

2.3. Interaction analysis between RID-B and GIGYF2

To confirm the interaction between GIGYF2 and RID-B, we performed a pull-down assay. Flag-tagged GIGYF2 was transiently expressed in HEK-293T cells (Fig. 3A), and the cellular lysates were incubated with Bio-RID-B- or biotin-immobilized resin. The bound proteins were then analyzed by Western blotting using an antibody against GIGYF2. Flag-tagged GIGYF2 was found to bind to Bio-RID-B-immobilized resin, but not to the control resin (Fig. 3B). We further elucidated the interaction and estimated the dissociation constant (K_D) between GIGYF2 and RID-B using surface plasmon resonance (SPR) analysis. We engineered a His-tagged truncated form of GIGYF2 corresponding to the 745–1030 region of GIGYF2 (GIGYF2(745–1030)) that is, the region displayed on the RID-B-binding phage (Fig. 3A and C). The recombinant protein was then purified to homogeneity. Various concentrations of GIGYF2(745–1030) were injected over the surface of the SA sensor chip on which Bio-RID-B had been immobilized through the interaction between biotin and avidin. GIGYF2(745–1030) bound to RID-B in a dose-dependent manner and global fitting gave a K_D value of 186 nM. These results indicate that RID-B strongly interacts with the 745–1030 a.a. region in GIGYF2 (Fig. 3D).

We also compared the affinity of the ridaifen analogs for GIGYF2. Previously, we synthesized several ridaifen derivatives and found that the cytotoxic activity of the ridaifen derivatives was dependent on its side chain.[8,9] Among them, RID-D ($\mathrm{Log}\,GI_{50}$ = −4.84 M) containing morpholine side chains showed low cytotoxicity with non-apoptotic activity in contrast to RID-B ($\mathrm{Log}\,GI_{50}$ = −5.93 M). In addition, no phage clone displaying GIGYF2 was acquired from a T7 phage display screen using Bio-RID-D (Table S1). Therefore, we speculated that the binding affinity between GIGYF2 and RID-D was less than that for RID-B. As shown in Figure 3B, we attempted the pull-down assay using Bio-RID-D and found that Bio-RID-B-immobilized resin bound to Flag-tagged GIGYF2 more strongly than Bio-RID-D-immobilized resin. Furthermore, SPR analysis showed that RID-B binds to GIGYF2(745–1030) at the range of concentrations tested (Fig. 3D and E). By contrast, little response was observed for RID-D, which is consistent with the results from the pull-down assay (Fig. 3F). Thus, the affinity of each ridaifen derivative for GIGYF2 correlated with the cytotoxicity data.

2.4. Effect of RID-B on the PI3K/Akt signaling pathway

Previous reports indicated that *GIGYF2* was a candidate gene for PARK11-linked Parkinson's disease. Furthermore, recent studies have reported the involvement of GIGYF2 in the PI3K/Akt signaling pathway,[21,22,31] and GIGYF2 was shown to be up-regulated in breast cancer cells in which high phosphorylation levels of Akt are observed. Thus we reasoned that the binding of RID-B to GIGYF2 might be biologically relevant. Initially, we examined whether RID-B affects the phosphorylation level of Akt. HEK293T cells transiently-expressing GIGYF2 were cultured in serum-free medium following pretreatment with RID-B for 4 h, and then stimulated with IGF-1 at different times. The phosphorylation of Akt at Ser473, which is known to be a representative marker for activation of Akt,[32–34] was detected by Western blot analysis using anti-phospho-Akt (Ser473) antibodies. As shown in Figure 4, the phosphorylation level of Akt at Ser473 15 min after IGF-1 stimulation was significantly reduced by RID-B in a dose-dependent manner. By contrast, there was no reduction in the phosphorylation level of Akt when the experiment was conducted using cells transfected with mock empty vector.

Taken together, our results demonstrate that RID-B directly binds to GIGYF2 and reduces the phosphorylation level of Akt at Ser473. This is the first report of a small molecule that binds to GIGYF2 to inhibit its function. Indeed, the knockdown of GIGYF2 reduced cell proliferation in breast cancer cell lines,[31] the RID-B-GIGYF2 interaction and subsequent inhibitory effect of the Akt phosphorylation may be relevant to the anti-proliferative activity of RID-B as well. Further experiments will clarify the detailed mode of actions.

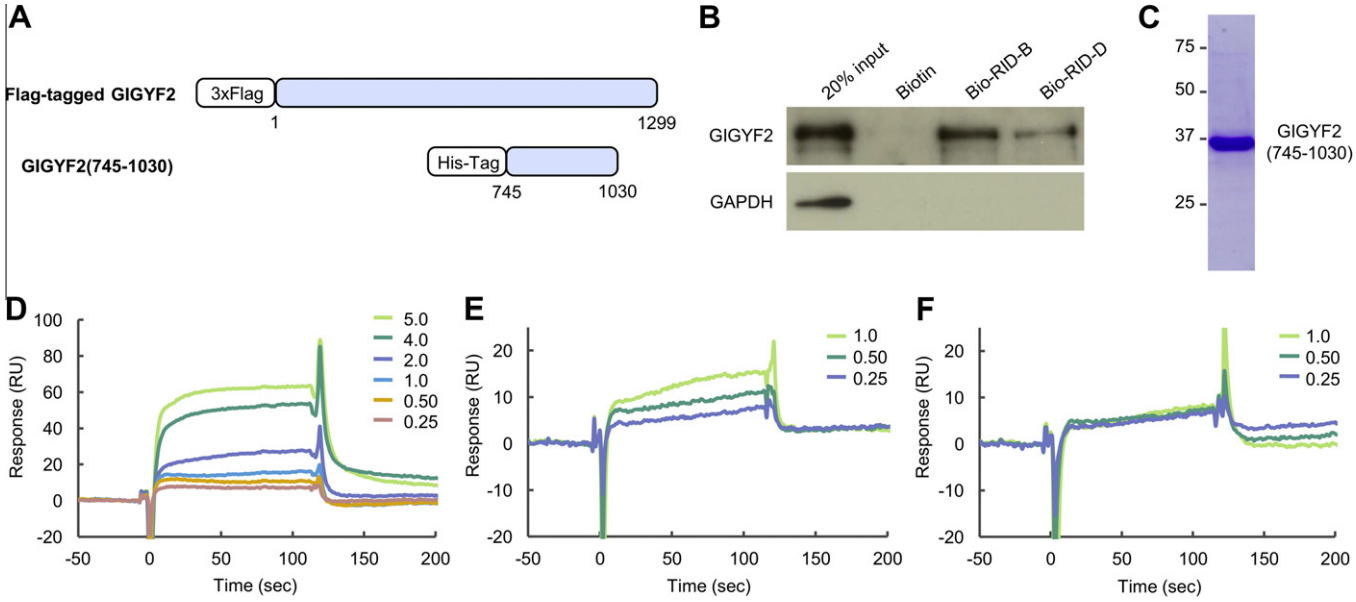

Figure 3. Direct interaction of RID-B with GIGYF2. (A) Schematic representation of the engineered full length or truncated GIGYF2 protein. (B) Interaction of RID-B or RID-D with Flag-tagged GIGYF2. Bio-RID-B, Bio-RID-D or biotin was fixed onto avidin beads and then incubated with cell extracts containing GIGYF2. After extensive washing, the bound GIGYF2 was detected by Western blot analysis. (C) Purified recombinant GIGYF2(745–1030). Recombinant GIGYF2(745–1030) from a bacterial expression system was purified to apparent homogeneity. The purity of the GIGYF2(745–1030) preparation was confirmed by SDS–PAGE analysis followed by staining with CBB. (D–F) A sensorgram obtained from SPR analysis between biotinylated ridaifen derivative and GIGYF2(745–1030). Bio-RID-B (D, E) or Bio-RID-D (F) was immobilized on a SA sensor chip. Solutions of purified GIGYF2(745–1030) at various concentrations (from top to bottom: 5.0, 4.0, 2.0, 1.0, 0.5 or 0.25 μM) was injected over the surface of the sensor chip. The binding responses (in RU) were recorded as a function of time (in sec). The estimated K_D value of interaction between RID-B and GIGYF2(745–1030) was 186 nM.

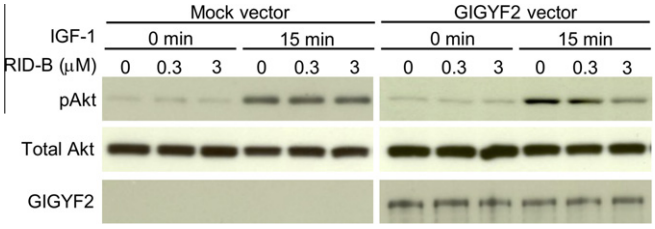

Figure 4. Effect of RID-B on the Akt phosphorylation in GIGYF2-overexpressing cells. HEK293T cells were transiently transfected with mock empty vector or Flag-GIGYF2 expression vector, and were serum-depleted for 20 h. Cells were then treated with 0, 0.3 or 3 μM of RID-B for 4 h followed by stimulation with IGF-1 for 0 or 15 min. Each protein was detected by Western blot analysis using a specific antibody. The data is a representative example from three independent experiments.

3. Conclusion

Our investigations have identified a small molecule that targets GIGYF2, which is involved in the PI3K/Akt signaling pathway and is up-regulated in breast cancer cells where Akt is highly phosphorylated. We employed a T7 phage display screen to identify RID-B-binding protein, a derivative of tamoxifen. Pull-down assay and SPR analysis confirmed the selective interaction between RID-B and GIGYF2. We also demonstrated that RID-B reduces the phosphorylation level of Akt in cells overexpressing GIGYF2. Taken together, our results show that RID-B directly binds to GIGYF2 and reduces the phosphorylation level of Akt at Ser473. Thus, binding of RID-B to GIGYF2 and subsequent reduction of Akt phosphorylation might explain the ER-independent anti-breast cancer activity of RID-B. Furthermore, RID-B and its analogs, as well as being valuable tools for investigating the molecular function of GIGYF2, could be important in the development of novel anti-breast cancer chemotherapy drugs.

4. Materials and methods

4.1. Chemistry

All reagents were purchased from Tokyo Kasei Kogyo Co., Ltd (TCI, Tokyo, Japan), Kanto Chemical Co., Inc. (Tokyo, Japan) or Sigma–Aldrich (St. Louis, MO), and used without further purification. 1-[3-(Benzyloxy)phenyl]propanone (**2**) was prepared from 3-benzyloxybenzaldehyde (Sigma–Aldrich) according to the literature method.[35–37] 2-Methyl-6-nitrobenzoic anhydride (MNBA) was purchased from Tokyo Kasei Kogyo Co., Ltd (M1439).

All melting points are uncorrected. ^{1}H and ^{13}C NMR spectra were recorded with chloroform (in chloroform-*d*) or methanol (in methanol-d_4) as an internal standard. Column chromatography was performed on silica gel 60 (Merck, Darmstadt, Germany). Thin layer chromatography was performed on Wakogel B5F. Unless otherwise stated, all reactions were carried out under an atmosphere of argon using dried glassware. Ammoniacal chloroform was prepared from 28% aqueous ammonia by ammonia extraction with chloroform.

4.2. Compounds

RID-B was synthesized chemically as described in previous reports.[8,9]

4.3. Antibodies

The following primary antibodies were used: rabbit polyclonal anti-GIGYF2 (H-95, Santa Cruz Biotechnology, Santa Cruz, CA), mouse monoclonal anti-GAPDH (6C5, Santa Cruz Biotechnology), rabbit polyclonal anti-Akt (Cell Signaling Technology, Tokyo, Japan), rabbit polyclonal anti-phospho-Akt (Ser473; Cell Signaling Technology).

4.4. Synthesis of Bio-RID-B and Bio-RID-D

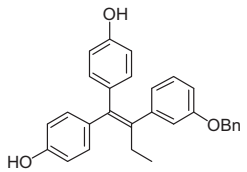

3

4.4.1. 2-[3-(Benzyloxy)phenyl]-1,1-bis(4-hydroxyphenyl)-1-butene (3)

To a suspension of zinc powder (15.8 g, 242 mmol) in THF (30 mL) at −10 °C was added titanium(IV) chloride (12.0 mL, 109 mmol). The reaction mixture was diluted with THF (20 mL) and refluxed at 90 °C (bath temperature) for 2 h and then a mixture of 4,4′-dihydroxybenzophenone (**1**) (12.3 g, 57.3 mmol) and 1-[3-(benzyloxy)phenyl]propanone (**2**) (4.30 g, 17.9 mmol) in THF (60 mL) was added to the mixture at 0 °C. After the reaction mixture had been refluxed at 90 °C (bath temperature) for 2 h in the dark, 10% aqueous potassium carbonate was added to the mixture at 0 °C in the light. The mixture was filtered through a short pad of Celite with ethyl acetate, and the filtrate was extracted with ethyl acetate. The organic layer was washed with brine, and dried over sodium sulfate. After filtration of the mixture and evaporation of the solvent, the crude product was purified by column chromatography on silica gel (eluant; hexane/ethyl acetate = 2:1) to afford **3** (7.09 g, 94%) as a colorless solid: mp: 153–156 °C; IR (KBr): 3402, 3039, 2962, 1589, 1504, 1234 cm^{-1}; ^1H NMR (CD_3OD): δ 7.36–7.26 (5H, m, Ar), 7.08–6.95 (1H, m, Ar), 7.02 (2H, d, J = 8.5 Hz, Ar), 6.76 (2H, d, J = 8.5 Hz, Ar), 6.73–6.67 (3H, m, Ar), 6.67 (2H, d, J = 9.0 Hz, Ar), 6.45 (2H, d, J = 9.0 Hz, Ar), 4.86 (2H, s, Bn), 2.46 (2H, q, J = 7.5 Hz, 3-H), 0.90 (3H, t, J = 7.5 Hz, 4-H); ^{13}C NMR (CD_3OD): δ 159.8, 157.2, 156.4, 145.6, 141.3, 140.1, 138.8 (Ar), 136.4 (1), 136.3 (2), 132.9, 131.6, 130.7, 129.8, 129.4, 128.7, 128.6, 123.5, 117.9, 116.1, 115.8, 115.2, 114.1 (Ar), 71.0 (Bn), 29.7 (3), 14.0 (4); HR MS: calcd for $C_{29}H_{26}O_3Na$ ($M+Na^+$) m/z 445.1774, found 445.1780.

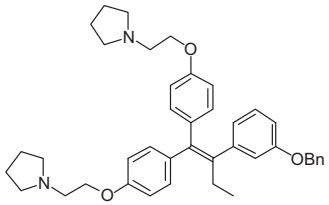

4

4.4.2. 2-[3-(Benzyloxy)phenyl]-1,1-bis{4-[2-(pyrrolidin-1-yl)ethoxy]phenyl}-1-butene (4)

To a solution of **3** (208 mg, 0.493 mmol) in DMF (4.93 mL) at 0 °C was added 60% sodium hydride (dispersion in paraffin liquid, 118 mg, 2.96 mmol). The reaction mixture was stirred for 15 min at 50 °C and then 1-(2-chloroethyl)pyrrolidine hydrochloride (278 mg, 1.63 mmol) was added in portions at room temperature. After the reaction mixture had been stirred for 3 h at 50 °C, saturated aqueous ammonium chloride was added at 0 °C. The mixture was extracted with dichloromethane, and the organic layer was washed with water and brine, and then dried over sodium sulfate. After filtration of the mixture and evaporation of the solvent, the crude product was purified by column chromatography on silica (eluant; ammoniacal chloroform/methanol = 9:1) to afford **4** (267 mg, 88%) as a pale yellow oil: IR (neat): 2962, 1604, 1512, 1242, 1041 cm^{-1}; ^1H NMR ($CDCl_3$): δ 7.40–7.28 (5H, m, Ar), 7.15–7.04 (3H, m, Ar), 6.91–6.70 (7H, m, Ar), 6.59–6.55 (2H, m, Ar), 4.88 (2H, s, Bn), 4.12 (2H, t, J = 6.0 Hz, OCH_2), 3.97 (2H, t, J = 6.0 Hz, OCH_2), 2.91 (2H, t, J = 6.0 Hz, NCH_2), 2.81 (2H, t, J = 6.0 Hz, NCH_2), 2.66–2.54 (8H, m, pyrrolidinyl 2-H), 2.46 (2H, q, J = 7.2 Hz, 3-H), 1.84–1.75 (8H, m, pyrrolidinyl 3-H), 0.93 (3H, t, J = 7.2 Hz, 4-H); ^{13}C NMR ($CDCl_3$): δ 158.3, 157.5, 156.7, 144.0, 140.7, 137.9, 137.1 (Ar), 136.2 (1), 135.8 (2), 131.7, 130.5, 129.6, 128.7, 128.4, 127.7, 127.4, 122.5, 116.3, 114.4, 114.0, 113.3, 112.7 (Ar), 69.8 (Bn), 66.9, 66.7 (OCH_2), 55.05, 55.00 (pyrrolidinyl 2-C), 54.64, 54.59 (NCH_2), 28.8 (3), 23.42, 23.38 (pyrrolidinyl 3-C), 13.6 (4); HR MS: calcd for $C_{41}H_{48}N_2O_3Na$ ($M+Na^+$) m/z 639.3557, found 639.3585.

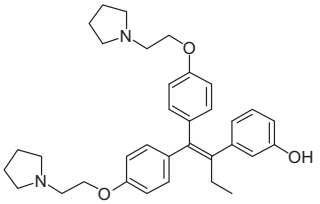

5

4.4.3. 2-(3-Hydroxyphenyl)-1,1-bis{4-[2-(pyrrolidin-1-yl)ethoxy]phenyl}-1-butene (5)

To a solution of **4** (109 mg, 0.177 mmol) in ethyl acetate (5.89 mL) at room temperature under an atmosphere of argon was added palladium on carbon (10% loading, 75.2 mg, 70.7 μmol). The reaction mixture was stirred for 4.5 h at room temperature under an atmosphere of hydrogen (1.0 atm) in the dark, and then transferred to an atmosphere of argon in the light. After filtration of the mixture through a short pad of Celite with ethyl acetate and evaporation of the solvent, the crude product was purified by thin layer chromatography on silica (eluant; ammoniacal chloroform/methanol = 9:1) to afford **5** (93.1 mg, 92%) as a pale yellow oil: IR (neat): 2970, 1604, 1512, 1242, 1049 cm^{-1}; ^1H NMR ($CDCl_3$): δ 7.08 (2H, d, J = 8.5 Hz, Ar), 6.96 (1H, dd, J = 8.0, 8.5 Hz, Ar), 6.84 (2H, d, J = 8.5 Hz, Ar), 6.76 (2H, d, J = 8.5 Hz, Ar), 6.60 (1H, d, J = 7.5 Hz, Ar), 6.53 (2H, dd, J = 2.0, 4.0 Hz, Ar), 6.47 (2H, d, J = 8.5 Hz, Ar), 4.12 (2H, t, J = 6.0 Hz, OCH_2), 3.91 (2H, t, J = 6.5 Hz, OCH_2), 2.93 (2H, t, J = 6.0 Hz, NCH_2), 2.80 (2H, t, J = 6.5 Hz, NCH_2), 2.69–2.62 (4H, m, pyrrolidinyl 2-H), 2.62–2.55 (4H, m, pyrrolidinyl 2-H), 2.39 (2H, q, J = 7.5 Hz, 3-H), 1.85–1.72 (8H, m, pyrrolidinyl 3-H), 0.87 (3H, t, J = 7.5 Hz, 4-H); ^{13}C NMR ($CDCl_3$): δ 157.3, 156.7, 156.5, 144.1, 141.0, 137.3 (Ar), 136.4 (1), 135.9 (2), 131.8, 130.6, 128.9, 121.0, 116.9, 113.9, 113.6, 113.2 (Ar), 66.5, 65.9 (OCH_2), 55.0, 54.9 (pyrrolidinyl 2-C), 54.6, 54.4 (NCH_2), 29.2 (3), 23.3, 23.2 (pyrrolidinyl 3-C), 13.6 (4); HR MS: calcd for $C_{34}H_{43}N_2O_3$ ($M+H^+$) m/z 527.3268, found 527.3247.

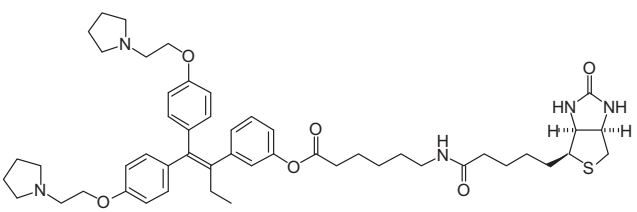

***N*-Biotinyl-6-aminohexanoic Acid Ridaifen B Ester (Bio-RID-B) (7)**

4.4.4. 2-[3-(*N*-Biotinyl-6-aminohexanoyl)phenyl]-1,1-bis{4-[2-(pyrrolidin-1-yl)ethoxy]phenyl}-1-butene (Bio-RID-B) (7)

To a solution of *N*-biotinyl-6-aminohexanoic acid (**6**) (20.0 mg, 56.0 μmol), 2-methyl-6-nitrobenzoic anhydride (MNBA) (23.1 mg, 67.1 μmol), 4-(dimethylamino)pyridine (DMAP) (1.37 mg, 11.2 μmol) and triethylamine (47.0 μL, 0.337 mmol) in dimethylformamide (DMF) (1.41 mL) at 0 °C was added a solution of **5** (35.4 mg, 67.2 μmol) in DMF (0.48 mL). After the reaction mixture had been stirred for 30 min at room temperature, it was concentrated by evaporation of the solvent and then the residue was purified by thin layer chromatography on silica (eluant; ammoniacal chloroform/methanol = 9:1) to afford **7** (33.9 mg, 70%) as a pale yellow oil: IR (neat): 3302, 2931, 1759, 1705, 1643, 1512, 1242, 1049 cm^{-1}; ^1H NMR ($CDCl_3$): δ 7.14–7.10 (3H, m, Ar), 6.92–6.86 (4H, m, Ar), 6.82 (1H, dd, J = 2.0, 8.0 Hz, Ar), 6.76 (2H, d, J = 9.0 Hz, Ar), 6.57 (2H, d, J = 9.0 Hz, Ar), 5.95–5.88 (1H, br m, 7″-NH), 5.83–5.72 (1H, br m, 8″-NH), 5.07–5.00 (1H, br m, 6′-NH), 4.48 (1H, dd, J = 5.5, 8.0 Hz, 8″-H), 4.30 (1H, dd, J = 4.5, 8.0 Hz, 7″-H), 4.12 (2H, t, J = 6.0 Hz, OCH_2), 3.98 (2H, t, J = 6.0 Hz, OCH_2), 3.28–3.25 (2H, m, 6′-H), 3.16–3.12 (1H, m, 6″-H), 2.91 (2H, t, J = 6.0 Hz, NCH_2), 2.89 (1H, dd, J = 5.5, 13.0 Hz, 9″-H), 2.82 (2H, t, J = 6.0 Hz, NCH_2), 2.71 (1H, d, J = 13.0 Hz, 9″-H), 2.67–2.61 (4H, m, pyrrolidinyl 2-H), 2.61–2.54 (4H, m, pyrrolidinyl 2-H), 2.51 (2H, t, J = 7.0 Hz, 2′-H), 2.46 (2H, q, J = 7.5 Hz, 3-H), 2.24–2.15 (2H, m, 2″-H), 1.85–1.62 (14H, m, pyrrolidinyl 3-H, 3′-H, 3″-H, 5″-H), 1.58–1.52 (2H, m, 5′-H), 1.47–1.38 (4H, m, 4′-H, 4″-H), 0.93 (3H, t, J = 7.5 Hz, 4-H); ^{13}C NMR ($CDCl_3$): δ 173.1 (1″), 172.0 (1′), 163.9 (urea), 157.6, 156.9, 150.4, 144.3, 139.7, 138.6 (Ar), 136.0 (1), 135.4 (2), 131.8, 130.4, 128.6, 127.5, 122.3, 119.0, 114.0, 113.5 (Ar), 67.0, 66.8 (OCH_2), 61.7 (7″), 60.1 (8″), 55.6 (6″), 55.10, 55.07 (pyrrolidinyl 2-C), 54.7, 54.6 (NCH_2), 40.5 (9″), 39.2 (6′), 36.0 (2″), 34.1 (2′), 29.2 (5′), 28.9 (3), 28.2 (4″), 28.1 (5″), 26.3 (4′), 25.7 (3″), 24.4 (3′), 23.45, 23.43 (pyrrolidinyl 3-C), 13.6 (4); HR MS: calcd for $C_{50}H_{68}N_5O_6S$ ($M+H^+$) m/z 866.4885, found 866.4842.

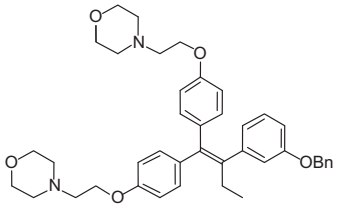

8

4.4.5. 2-[3-(Benzyloxy)phenyl]-1,1-bis{4-[2-(morpholin-4-yl)ethoxy]phenyl}-1-butene (8)

A dispersion of sodium hydride in paraffin liquid (60%, 287 mg, 7.17 mmol) was washed with petroleum ether under an atmosphere of argon. A solution of **3** (501 mg, 1.18 mmol) in DMF (12.0 mL) was then added to the resulting sodium hydride at 0 °C. The reaction mixture was stirred for 15 min at room temperature and then 4-(2-chloroethyl)morpholin hydrochloride (724 mg, 3.89 mmol) was added to the suspension in portions at room temperature. After the reaction mixture had been stirred for 6 h at 50 °C, saturated aqueous ammonium chloride was added at 0 °C. The mixture was extracted with dichloromethane, and the organic layer was washed with water and brine, and dried over sodium sulfate. After filtration of the mixture and evaporation of the solvent, the crude product was purified by column chromatography on silica (eluant; chloroform/methanol = 20:1) to afford **8** (734 mg, 96%) as a pale yellow oil: IR (neat): 2958, 1603, 1507, 1243, 1033 cm^{-1}; ^1H NMR ($CDCl_3$): δ 7.37 (4H, d, J = 3.5 Hz, Ar), 7.33–7.30 (1H, m, Ar), 7.13 (2H, d, J = 8.5 Hz, Ar), 7.07 (1H, t, J = 8.0 Hz, Ar), 6.88 (2H, d, J = 8.5 Hz, Ar), 6.77 (2H, d, J = 9.0 Hz, Ar), 6.75–6.71 (3H, m, Ar), 6.56 (2H, d, J = 8.5 Hz, Ar), 4.89 (2H, s, Bn), 4.13 (2H, t, J = 5.5 Hz, OCH_2), 3.98 (2H, t, J = 5.5 Hz, OCH_2), 3.75 (4H, t, J = 4.5 Hz, morpholinyl OCH_2), 3.69 (4H, t, J = 4.5 Hz, morpholinyl OCH_2), 2.82 (2H, t, J = 5.5 Hz, NCH_2), 2.72 (2H, t, J = 5.5 Hz, NCH_2), 2.59 (4H, t, J = 4.5 Hz, morpholinyl NCH_2), 2.52 (4H, t, J = 4.5 Hz, morpholinyl NCH_2), 2.45 (2H, q, J = 7.5 Hz, 3-H), 0.93 (3H, t, J = 7.5 Hz, 4-H); ^{13}C NMR ($CDCl_3$): δ 158.4, 157.4, 156.7, 144.0, 140.9, 137.9, 137.1 (Ar), 136.4 (1), 136.0 (2), 131.8, 130.6, 128.8, 128.5, 127.8, 127.5, 122.6, 116.4, 114.1, 113.4, 112.8 (Ar), 70.0 (Bn), 66.94, 66.89 (OCH_2), 65.7, 65.5 (morpholinyl 2-C), 57.72, 57.67 (morpholinyl 3-C), 54.10, 54.07 (NCH_2), 28.9 (3), 13.6 (4); HR MS: calcd for $C_{41}H_{48}N_2O_5$-Na ($M+Na^+$) m/z 671.3455, found 671.3489.

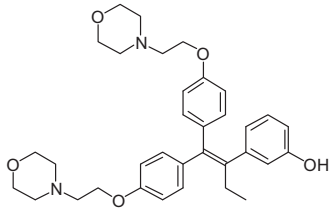

9

4.4.6. 2-(3-Hydroxyphenyl)-1,1-bis{4-[2-(morpholin-4-yl)ethoxy]phenyl}-1-butene (9)

To a solution of **8** (734 mg, 1.13 mmol) in ethyl acetate (32.0 mL) at room temperature under an atmosphere of argon was added palladium on carbon (10% loading, 532 mg, 0.500 mmol). The reaction mixture was stirred for 48 h at room temperature under an atmosphere of hydrogen (1.0 atm) in the dark, and then transferred to an atmosphere of argon in the light. After filtration of the mixture through a short pad of Celite with ethyl acetate and evaporation of the solvent, the residue was diluted with ethyl acetate (32.0 mL) at room temperature under an atmosphere of argon. Palladium on carbon (10% loading, 269 mg, 0.253 mmol) was added to the reaction mixture, which was then stirred for 48 h at room temperature under an atmosphere of hydrogen (1.0 atm) in the dark. The reaction mixture was subsequently transferred to an atmosphere of argon in the light. After filtration of the mixture through a short pad of Celite with ethyl acetate and evaporation of the solvent, the crude product was purified by column chromatography on silica (eluant; chloroform/methanol = 18:1) to afford **9** (507 mg, 80%) as a colorless solid: mp: 51–52 °C; IR (neat): 2959, 1605, 1509, 1243, 1035 cm^{-1}; ^1H NMR ($CDCl_3$): δ 7.11 (2H, d, J = 8.5 Hz, Ar), 7.03 (1H, t, J = 8.0 Hz, Ar), 6.87 (2H, d, J = 10.0 Hz, Ar), 6.77 (2H, d, J = 8.5 Hz, Ar), 6.67 (1H, d, J = 7.5 Hz, Ar), 6.58–6.53 (4H, m, Ar), 4.13 (2H, t, J = 5.5 Hz, OCH_2), 3.97 (2H, t, J = 5.5 Hz, OCH_2), 3.74 (4H, t, J = 4.5 Hz, morpholinyl OCH_2), 3.70 (4H, t, J = 4.5 Hz, morpholinyl OCH_2), 2.82 (2H, t, J = 5.5 Hz, NCH_2), 2.71 (2H, t, J = 5.5 Hz, NCH_2), 2.60 (4H, t, J = 4.5 Hz, morpholinyl NCH_2), 2.53 (4H, t, J = 4.5 Hz, morpholinyl NCH_2), 2.43 (2H, q, J = 7.5 Hz, 3-H), 0.92 (3H, t, J = 7.5 Hz, 4-H); ^{13}C NMR ($CDCl_3$): δ 157.4, 156.7, 155.3, 144.4, 140.7, 137.8 (Ar), 136.4 (1), 135.9 (2), 131.8, 130.6, 129.0, 122.2, 116.7, 114.1, 113.4, 113.1 (Ar), 66.9, 66.8 (OCH_2), 65.7, 65.3 (morpholinyl 2-C), 57.73, 57.65 (morpholinyl 3-C), 54.1, 54.0 (NCH_2), 29.1 (3), 13.6 (4); HR MS: calcd for $C_{34}H_{43}N_2O_5$ ($M+H^+$) m/z 559.3166, found 559.3148: calcd for $C_{34}H_{42}N_2O_5Na$ ($M+Na^+$) m/z 581.2986, found 581.2978.

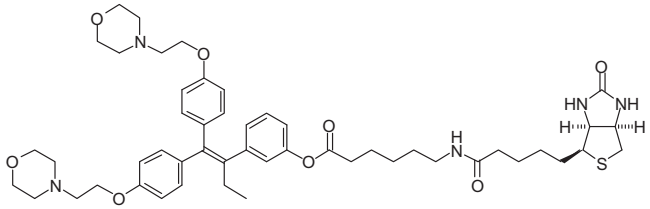

***N*-Biotinyl-6-aminohexanoic Acid Ridaifen D Ester (Bio-RID-D) (10)**

4.4.7. 2-[3-(*N*-Biotinyl-6-aminohexanoyl)phenyl]-1,1-bis{4-[2-(morpholin-4-yl)ethoxy]phenyl}-1-butene (Bio-RID-D) (10)

To a solution of *N*-biotinyl-6-aminohexanoic acid (**6**) (16.0 mg, 44.8 μmol), 2-methyl-6-nitrobenzoic anhydride (MNBA) (18.5 mg, 53.7 μmol), 4-(dimethylamino)pyridine (DMAP) (1.09 mg, 8.92 μmol) and triethylamine (37.4 μL, 0.268 mmol) in dimethylformamide (DMF) (1.34 mL) at 0 °C was added a solution of **9** (30.0 mg, 53.7 μmol) in DMF (0.45 mL). After the reaction mixture had been stirred for 1.5 h at room temperature, it was concentrated by evaporation of the solvent and then the residue was purified by thin layer chromatography on silica (eluant; ammoniacal chloroform/methanol = 9:1) to afford **10** (28.4 mg, 72%) as a pale yellow oil: IR (neat): 3303, 2927, 1765, 1708, 1643, 1507, 1243, 1039 cm^{-1}; ^1H NMR ($CDCl_3$): δ 7.13–7.10 (3H, m, Ar), 6.90–6.75 (7H, m, Ar), 6.55 (2H, d, J = 9.0 Hz, Ar), 6.45–6.27 (1H, br m, 7″-NH), 6.18–6.06 (1H, br m, 8″-NH), 5.53–5.36 (1H, br m, 6′-NH), 4.47 (1H, dd, J = 4.5, 7.5 Hz, 8″-H), 4.29 (1H, dd, J = 5.0, 7.0 Hz, 7″-H), 4.12 (2H, t, J = 5.5 Hz, OCH_2), 3.97 (2H, t, J = 5.5 Hz, OCH_2), 3.73 (4H, t, J = 5.0 Hz, morpholinyl OCH_2), 3.69 (4H, t, J = 5.0 Hz, morpholinyl OCH_2), 3.24 (2H, dd, J = 6.0, 7.5 Hz, 6′-H), 3.13 (1H, dd, J = 4.5, 7.5 Hz, 6″-H), 2.88 (1H, dd, J = 4.5, 13.5 Hz, 9″-H), 2.81 (2H, t, J = 5.5 Hz, NCH_2), 2.72–2.69 (3H, m, NCH_2, 9″-H), 2.58 (4H, t, J = 5.0 Hz, morpholinyl NCH_2), 2.53–2.50 (6H, m, morpholinyl NCH_2, 2′-H), 2.45 (2H, q, J = 8.0 Hz, 3-H), 2.19 (2H, t, J = 7.0 Hz, 2″-H), 1.76–1.63 (6H, m, 3′-H, 3″-H, 5″-H), 1.57–1.52 (2H, m, 5′-H), 1.47–1.38 (4H, m, 4′-H, 4″-H), 0.93 (3H, t, J = 8.0 Hz, 4-H); ^{13}C NMR ($CDCl_3$): δ 173.1 (1″), 172.0 (1′), 163.8 (urea), 157.5, 156.8, 150.5, 144.2, 139.9, 138.5 (Ar), 136.1 (1), 135.5 (2), 131.8, 130.5, 128.7, 127.5, 122.3, 119.0, 114.1, 113.5 (Ar), 66.92, 66.87 (OCH_2), 65.7, 65.6 (morpholinyl 2-C), 61.7 (7″), 60.1 (8″), 57.7, 57.6 (morpholinyl 3-C), 55.6 (6″), 54.1, 54.0 (NCH_2), 40.5 (9″), 39.2 (6′), 36.0 (2″), 34.1 (2′), 29.3 (5′), 28.9 (3), 28.2 (4″), 28.1 (5″), 26.3 (4′), 25.7 (3″), 24.4 (3′), 13.6 (4); HR MS: calcd for $C_{50}H_{68}N_5O_8S$ ($M+H^+$) m/z 898.4783, found 898.4740: calcd for $C_{50}H_{67}N_5O_8SNa$ ($M+Na^+$) m/z 920.4603, found 920.4615.

4.5. T7 phage display screen

Unless stated otherwise, all manipulations were performed at room temperature. A 10 μM of Bio-RID-B solution was added to a streptavidin-coated 96-well microplate (Nalge Nunc International, Wiesbaden, Germany) and incubated for 1 h. The wells were then blocked with 3% skimmed milk in TBS (25 mM Tris–HCl, 137 mM NaCl, 2.7 mM KCl, pH 7.4) for 1 h. An aliquot of the T7 phage library constructed from cDNA of Jurkat cells was added to each well and the mixture was then incubated for 1 h. After incubation, the wells were washed 10 times with TBST (TBS, 0.1% Tween 20). An elution buffer (TBS, 1% SDS) was then added and the mixture incubated for 15 min to recover the remaining phage particles. In order to amplify the recovered phage particles, each eluate was mixed with a culture of *Esherishia coli* BLT5615 (Merck) at a MOI of 0.001. The cells were then cultured at 37 °C until cell lysis was observed. The resulting solution was used for the next round of biopanning. After four rounds of selection, the eluate was mixed with 1 mL of BLT5615 culture and 10 mL of warmed top agarose and then poured evenly across the surface of an LB/carbenicillin plate. Once the overlay had solidified, the plate was incubated at 37 °C for 3 h in order to allow the formation of phage plaques. A total of 15 plaques were randomly picked and each plaque was suspended in 100 mM NaCl, 6 mM $MgSO_4$, 20 mM Tris–HCl pH 8.0. The DNA sequence of each phage clone was then analyzed as described in a previous report.[16]

4.6. Similarity search

A similarity scores were obtained by FASTA (http://www.ebi.ac.uk/Tools/sss/fasta/).

4.7. Construction of expression vectors

The phage clone displaying 745–1030 a.a. of GIFYF2 was used as a template for the PCR. DNA encoding GIGYF2(745–1030) was amplified using the following primer set: forward, 5′-CATATGG AAATGAGGGCAAAA-3′, and reverse, 5′-CTCGAGTCAACGAGCTCTG TTTGGTTGCT-3′ (underlined bases highlight the restriction endonuclease recognition sites). The PCR product was inserted into pET-28a (+) (Merck) expression vector in-frame with a His-tag at the N-terminus. A full-length GIGYF2 cDNA clone was purchased from Kazusa DNA Research Institute (Gene No. KIAA0642, Chiba, Japan) and the plasmid DNA was used as template for the PCR. The full-length GIGYF2 cDNA was constructed using the following primer set: forward, 5′-GCGGCCGCGGCAGCGGAAACGCAGACACT-3′, and reverse, 5′-GGATCCTCAGTAGTCATCCAACGTCTCGATTTC-3′. The PCR product was inserted into p3xFLAG-CMV-10 (Sigma–Aldrich) expression vector in-frame with 3× FLAG-tag at the N-terminus.

4.8. Expression and purification of recombinant GIGYF2(745–1030)

The engineered GIGYF2(745–1030) expression vector was used to transform *E. coli* Rosetta 2 (DE3)plysS (Merck). These bacteria were grown in LB medium containing 30 μg/mL of kanamycin and 100 μg/mL of chloramphenicol at 37 °C until the OD_{600} reached 0.5 before addition of 1 mM isopropyl thio-β-D-galactoside (IPTG). The cells were then incubated for a further 4 h at 37 °C. After incubation, the cells were harvested and suspended in elution buffer I (50 mM Na_2HPO_4, 5% glycerol, 0.05% Triton X-100, pH 7.2) containing protease inhibitor cocktail (Nacalai Tesque, Kyoto, Japan). The cells were disrupted by sonication and the resulting extract was clarified by centrifugation (17,500*g*) at 4 °C for 10 min. Solid ammonium sulfate was then gradually added to the clarified cell-free extract to a final concentration of 40% mass/volume. The solution was stirred at 4 °C for 30 min and the final precipitate was pelleted by centrifugation (17,500*g*) at 4 °C for 10 min and then resuspended in binding buffer I (0.5 M $(NH_4)_2SO_4$, 50 mM Na_2HPO_4, 5% glycerol, 0.05% Triton X-100, pH 7.2). Recombinant GIGYF2(745–1030) was further purified by loading the sample onto a HiTrap Phenyl HP column (1 mL, GE Healthcare UK Ltd, Buckinghamshire, UK) equilibrated in binding buffer I using an FPLC system (GE Healthcare). The bound protein was subsequently eluted with elution buffer I. Fractions containing GIGYF2(745–1030) were pooled and loaded onto a HisTrap HP column (1 mL, GE Healthcare) equilibrated in binding buffer II (7.8 mM Na_2HPO_4, 2.7 mM KCl, 1.5 mM KH_2PO_4, 0.5 M NaCl, 5% glycerol, 0.05% Triton X-100, pH 7.4) using an FPLC system. Finally, bound proteins were eluted using elution buffer II (binding buffer II plus 0.5 M imidazole).

4.9. Surface plasmon resonance assay

SPR analysis was performed on a Biacore® 3000 (GE Healthcare). The purified GIGYF2(745–1030) was buffer exchanged into PBS (67 mM Na_2HPO_4, 12.5 mM KH_2PO_4, 70 mM NaCl, pH 7.4) and the concentration was quantified using DC protein assay kit (Bio-Rad Laboratories, Hercules, CA). Solutions of bovine serum albumin (BSA) at different concentrations were used as standards for this assay. After immobilization of Bio-RID-B and biotin on an SA sensor chip, appropriate concentrations of GIGYF2(745–1030)

were injected over the flow cells. Binding analyses were carried out in PBS at a flow rate of 20 μL/min at 25 °C. The bulk effects of DMSO were subtracted using reference flow cells. Kinetic parameters were determined by analyzing the data using BIAevaluation 4.1 software (GE Healthcare).

4.10. Western blot analysis

Protein samples were separated by SDS–polyacrylamide gel electrophoresis (SDS–PAGE) and transferred from the gel to a polyvinylidene difluoride membrane (Merck) by electroblotting. After blocking for 1 h, proteins were detected by Western blot using primary antibody at the appropriate dilution and horseradish peroxidase-conjugated anti-rabbit or anti-mouse IgG (GE Healthcare) as the secondary antibody. The chemiluminescence was performed using ECL western blotting detection reagents (GE Healthcare) or ECL prime western blotting detection reagent (GE Healthcare).

4.11. Cell culture and transfection

HEK293T cells were maintained in DMEM (Nacalai Tesque) supplemented with 10% fetal bovine serum (Life Technologies, Carlsbad, CA) and 1% Penicillin–Streptomycin Mixed Solution (Nacalai Tesque) at 37 °C under a humidified atmosphere of 5% CO_2. Transient transfection was performed using the X-tremeGENE HP DNA Transfection Reagent (Roche Diagnostics, Indianapolis, IN) according to the manufacturer's instructions.

4.12. Pull-down assay

Twenty-four hours before transfection, HEK293T cells were seeded at 2.5×10^5 cells per well in 6-well plates. Twenty-four hours after transfection with 1 μg of the Flag-tagged GIGYF2 expression vector, the cells from all the wells were harvested in 200 μL 1% Triton lysis buffer (10 mM Tris–HCl pH 7.4, 5 mM EDTA, 1% Triton X-100, protease inhibitor cocktail). The cell lysate was incubated on ice for 1 h and the soluble fraction was then obtained by centrifugation (17,500*g*) at 4 °C for 30 min. The soluble fraction was subsequently diluted by addition of 0.1% Triton buffer with TBS. Avidin–agarose beads (Sigma–Aldrich) were incubated with 10 μM of Bio-RID-B or DMSO and then washed to remove unbound compounds. A 500 μL aliquot of the diluted soluble fraction was then mixed with the avidin–agarose beads at 4 °C for 4 h. The beads were washed 6 times with wash buffer (0.1% Triton buffer in TBS) and the bound proteins were subsequently eluted with 2× SDS sample buffer (100 mM Tris–HCl pH 6.8, 4% SDS, 20% glycerol, 12% β-mercaptoethanol, bromophenol blue). Samples were incubated at 96 °C for 10 min and analyzed by Western blot using antibodies against GIGYF2 (or GAPDH as a control).

4.13. Analysis of the phosphorylation level of Akt

Twenty-four hours before transfection, HEK293T cells were seeded at 2.5×10^5 cells per well in 6-well plates. The cells were transiently transfected with 1 μg of mock empty vector or Flag-tagged GIGYF2 expression vector. Thirty-six hours after transfection, cells were cultured in serum-free medium for 20 h and then incubated with 0, 0.3 or 3 μM (0.1% DMSO) for 4 h following stimulation with 100 ng/mL of IGF-1 (GenScript USA, Piscataway, NJ) for 0 or 15 min. Cells were harvested in 1% Triton lysis buffer containing protease inhibitor cocktail (EDTA-free) and phosphatase inhibitor cocktail (Thermo Fisher Scientific, Waltham, MA) and then the lysates were placed on ice for 1 h. After centrifugation (17,500*g*) at 4 °C for 30 min, the concentration of supernatant was quantified using DC protein assay kit with BSA standards. The supernatant was diluted to 2 mg/mL with 1% Triton lysis buffer and mixed with an equal volume of 2× SDS sample buffer so that the final protein concentration of the sample was 1 mg/mL. The sample was then incubated at 96 °C for 10 min. The data was analyzed by Western blot using antibodies against Akt, phosphorylated Akt or GIGYF2.

Acknowledgment

This study was partially supported by a Health Labour Sciences Research Grant from the Ministry of Health Labour and Welfare, Japan.

Supplementary data

Supplementary data associated with this article can be found, in the online version, at http://dx.doi.org/10.1016/j.bmc.2012.10.037.

References and notes

1. Dhingra, K. *Invest. New Drugs* **1999**, *17*, 285.
2. Fisher, B.; Costantino, J. P.; Wickerham, D. L.; Redmond, C. K.; Kavanah, M.; Cronin, W. M.; Vogel, V.; Robidoux, A.; Dimitrov, N.; Atkins, J.; Daly, M.; Wieand, S.; Tan-Chiu, E.; Ford, L.; Wolmark, N. *J. Natl. Cancer Inst.* **1998**, *90*, 1371.
3. Mandlekar, S.; Kong, A. N. *Apoptosis* **2001**, *6*, 469.
4. Ferlini, C.; Scambia, G.; Marone, M.; Distefano, M.; Gaggini, C.; Ferrandina, G.; Fattorossi, A.; Isola, G.; Benedetti Panici, P.; Mancuso, S. *Br. J. Cancer* **1999**, *79*, 257.
5. Kang, Y.; Cortina, R.; Perry, R. R. *J. Natl. Cancer Inst.* **1996**, *88*, 279.
6. Catherino, W. H.; Jordan, V. C. *Drug Saf.* **1993**, *8*, 381.
7. Dorssers, L. C.; Van der Flier, S.; Brinkman, A.; van Agthoven, T.; Veldscholte, J.; Berns, E. M.; Klijn, J. G.; Beex, L. V.; Foekens, J. A. *Drugs* **2001**, *61*, 1721.
8. Shiina, I.; Sano, Y.; Nakata, K.; Kikuchi, T.; Sasaki, A.; Ikekita, M.; Hasome, Y. *Bioorg. Med. Chem. Lett.* **2007**, *17*, 2421.
9. Shiina, I.; Sano, Y.; Nakata, K.; Kikuchi, T.; Sasaki, A.; Ikekita, M.; Nagahara, Y.; Hasome, Y.; Yamori, T.; Yamazaki, K. *Biochem. Pharmacol.* **2008**, *75*, 1014.
10. Nagahara, Y.; Shiina, I.; Nakata, K.; Sasaki, A.; Miyamoto, T.; Ikekita, M. *Cancer Sci.* **2008**, *99*, 608.
11. Sche, P. P.; McKenzie, K. M.; White, J. D.; Austin, D. *J. Chem. Biol.* **1999**, *6*, 707.
12. Smith, G. P.; Petrenko, V. A. *Chem. Rev.* **1997**, *97*, 391.
13. Takakusagi, Y.; Takakusagi, K.; Sugawara, F.; Sakaguchi, K. *Expert Opin. Drug Discov.* **2010**, *5*, 361.
14. Manita, D.; Toba, Y.; Takakusagi, Y.; Matsumoto, Y.; Kusayanagi, T.; Takakusagi, K.; Tsukuda, S.; Takada, K.; Kanai, Y.; Kamisuki, S.; Sakaguchi, K.; Sugawara, F. *Bioorg. Med. Chem.* **2011**, *19*, 7690.
15. Matsumoto, Y.; Shindo, Y.; Takakusagi, Y.; Takakusagi, K.; Tsukuda, S.; Kusayanagi, T.; Sato, H.; Kawabe, T.; Sugawara, F.; Sakaguchi, K. *Bioorg. Med. Chem.* **2011**, *19*, 7049.
16. Morohashi, K.; Sahara, H.; Watashi, K.; Iwabata, K.; Sunoki, T.; Kuramochi, K.; Takakusagi, K.; Miyashita, H.; Sato, N.; Tanabe, A.; Shimotohno, K.; Kobayashi, S.; Sakaguchi, K.; Sugawara, F. *PLoS One* **2011**, *6*, e18285.
17. Saitoh, T.; Kuramochi, K.; Imai, T.; Takata, K.; Takehara, M.; Kobayashi, S.; Sakaguchi, K.; Sugawara, F. *Bioorg. Med. Chem.* **2008**, *16*, 5815.
18. Takakusagi, K.; Takakusagi, Y.; Ohta, K.; Aoki, S.; Sugawara, F.; Sakaguchi, K. *Protein Eng Des. Sel.* **2010**, *23*, 51.
19. Takami, M.; Takakusagi, Y.; Kuramochi, K.; Tsukuda, S.; Aoki, S.; Morohashi, K.; Ohta, K.; Kobayashi, S.; Sakaguchi, K.; Sugawara, F. *Molecules* **2011**, *16*, 4278.
20. Miyano, Y.; Tsukuda, S.; Sakimoto, I.; Takeuchi, R.; Shimura, S.; Takahashi, N.; Kusayanagi, T.; Takakusagi, Y.; Okado, M.; Matsumoto, Y.; Takakusagi, K.; Takeuchi, T.; Kamisuki, S.; Nakazaki, A.; Ohta, K.; Miura, M.; Kuramochi, K.; Mizushina, Y.; Kobayashi, S.; Sugawara, F.; Sakaguchi, K. *Bioorg. Med. Chem.* **2012**, *20*, 3985.
21. Ajiro, M.; Katagiri, T.; Ueda, K.; Nakagawa, H.; Fukukawa, C.; Lin, M. L.; Park, J. H.; Nishidate, T.; Daigo, Y.; Nakamura, Y. *Int. J. Oncol.* **2009**, *35*, 673.
22. Giovannone, B.; Lee, E.; Laviola, L.; Giorgino, F.; Cleveland, K. A.; Smith, R. J. *J. Biol. Chem.* **2003**, *278*, 31564.
23. Mukaiyama, T. *Angew. Chem., Int. Ed.* **1977**, *16*, 817.
24. Yu, D. D.; Forman, B. M. *J. Org. Chem.* **2003**, *68*, 9489.
25. Shiina, I.; Ibuka, R.; Kubota, M. *Chem. Lett.* **2002**, *31*, 286.
26. Shiina, I.; Kubota, M.; Oshiumi, H.; Hashizume, M. *J. Org. Chem.* **2004**, *69*, 1822.
27. Shiina, I.; Fukui, H.; Sasaki, A. *Nat. Protoc.* **2007**, *2*, 2312.

28. 1-[3-(Benzyloxy)phenyl]propanone (**2**) was prepared from 3-benzyloxybenzaldehyde according to the literature method. See the references in the experimental Section 4.1.
29. Wilchek, M.; Bayer, E. A. *Methods Enzymol.* **1990**, *184*, 123.
30. Elia, G. *Proteomics* **2008**, *8*, 4012.
31. Ajiro, M.; Nishidate, T.; Katagiri, T.; Nakamura, Y. *Int. J. Oncol.* **2010**, *37*, 1085.
32. Alessi, D. R.; Andjelkovic, M.; Caudwell, B.; Cron, P.; Morrice, N.; Cohen, P.; Hemmings, B. A. *EMBO J.* **1996**, *15*, 6541.
33. Scheid, M. P.; Marignani, P. A.; Woodgett, J. R. *Mol. Cell. Biol.* **2002**, *22*, 6247.
34. Yang, J.; Cron, P.; Thompson, V.; Good, V. M.; Hess, D.; Hemmings, B. A.; Barford, D. *Mol. Cell* **2002**, *9*, 1227.
35. Cheng, H. M.; Casida, J. E. *J. Agric. Food Chem.* **1973**, *21*, 1037.
36. Rastogi, S. N.; Anand, N.; Gupta, P. P.; Sharma, J. N. *J. Med. Chem.* **1973**, *16*, 797.
37. Maguire, J. H.; Kraus, B. L.; Butler, T. C.; Dudley, K. H. *Drug Metab. Dispos.* **1981**, *9*, 393.